3D printing of synthetic rubber ink via the direct ink writing process

by Sarath Suresh Kamath and Jae-Won Choi, The University of Akron

Natural rubber, which is mainly composed of poly-cis-isoprene and is produced by the rubber tree (*Hevea brasiliensis*), has been used for many applications in the automotive industry because it provides a broad range of physical and chemical properties. In the 1890s, there was a surge in demand for rubber to use for pneumatic tires for automobiles. However, as the performance of natural rubber is limited in terms of thermal stability, chemical resistance and oil resistance (ref. 1), efforts were made to create an artificial elastomer that could be synthesized from petroleum by-products. Bayer AG in Germany succeeded in polymerizing isoprene, the first synthetic rubber, in its laboratory in early 1906 (ref. 2). The first rubber polymer, butadiene, was developed at I.G. Farben in 1929, and this polymer provided the foundation for the first large scale commercial production of synthetic rubber (ref. 3). As the United States was expanding the manufacture of synthetic rubber during World War II, the U.S. government launched a major effort to improve synthetic rubber and increase its production (ref. 4).

Of the synthetic rubber materials used in the automotive industry, the most prevalent synthetic rubber is styrene-butadiene rubber (SBR), which is derived from the copolymerization of styrene and 1,3-butadiene. SBR, and latex made using SBR, have a broad range of physical and chemical properties, and they share a number of advantages over natural rubber: They are less expensive, are resistant to abrasion, have better aging characteristics and contain no allergens. SBR latexes, with the help of compounding technology, can be designed or tailored to give optimum end results for general and special purpose products (ref. 5).

Conventional tire manufacturing methods employ vulcanization at high temperature and high pressure to process synthetic rubber, as well as customized machinery dies and molds to fabricate each product, and the manufacturing methods are conducted on a huge scale. Because of this, conventional methods cannot be used to create customized synthetic rubber parts in small batches. One potential method that might be used to produce such parts is additive manufacturing (AM). This method, which is also known as three-dimensional (3D) printing, was first developed in the mid-1980s to produce custom designed products using materials such as polymers, ceramics and metals. Additive manufacturing is the sequential layer by layer process of joining materials using computer control to create various three-dimensional objects (refs. 6 and 7). As 3D printers are able to produce complex structures with optimized physical properties, additive manufacturing has drawn tremendous attention from researchers in different fields, and has been used in numerous applications in the aerospace (ref. 8) and automotive industries (ref. 9), as well as for architectural purposes (ref. 10). Additive manufacturing is superior to traditional manufacturing in terms of customization and its ability to produce structures having complex geometries with less material waste and without the need for specialized tools (refs. 11 and 12).

Direct ink writing (DIW) 3D printing, also called direct print (DP), has been employed in recent years to print complex 3D objects through the layer by layer deposition of printable inks. Generally, the direct ink writing process describes the fabrication method that employs a computer controlled translation stage, which moves a pattern generating device (i.e., an ink deposition nozzle) to create materials with controlled architecture and composition. The printer can precisely manipulate the extrusion of fluidic inks through a nozzle to print the designs (refs. 13 and 14). Printable inks are a key component in direct ink writing, as they determine not only the possible printable geometries, but also the internal structure and performance of the printed objects (ref. 15). Direct ink writing relies on the careful preparation of inks with ideal rheological properties (the properties that describe the deformation and flow of the inks during the printing process) to achieve successful fabrication of 3D structures.

Because rubber materials have excellent mechanical properties, very high elongation at break and good impact resilience, they are indispensable in many everyday areas of application. Rubber compounding is widely used in the rubber manufacturing industries to produce tires, latex gloves, rubber bearings, dock fenders, protective clothing, footwear, and many other products. However, this material has limitations for additive manufacturing applications because of the high temperature and pressure required during processing. Although additive manufacturing technologies have been disseminated and utilized as mature technologies, there is still no standard technical solution for the additive manufacturing printing of rubber inks that can withstand vulcanization.

In recent years, Maria et al. printed elastomeric latex materials using an inkjet process (ref. 16), and Miguel et al. printed natural rubber latex using a customized inkjet printer (ref. 17). Inkjet printing of latex is known to have several drawbacks, and one that is particularly notable is nozzle clogging and agglomeration, which could result from efforts to control the material's viscosity to facilitate its use for latex printing. Later, Philip et al. printed synthetic latex using a vat photopolymerization process (ref. 18) in which a supporting hydrogel scaffold system surrounds the latex particles. This technique also has limitations in terms of the photocuring process, and only materials within a narrow range of viscosity can be printed. In addition, the part printed using this method also exhibited a ~40 vol% shrinkage because of a large volume of solvent in the latex, even though the material has been photopolymerized. Recently, rubber inks with a high solid content were introduced by Kim and Choi (ref. 19), who used natural rubber latex as the matrix to ensure that the rubber ink would be suitable for use in the direct print process. They were able to maintain a sufficiently high solid content by preparing rubber inks with different ratios of synthetic rubber and natural latex, and the study demonstrated the feasibility of using the developed rubber ink

for additive manufacturing.

In this article, a blend of SBR latex and butadiene rubber latex was prepared as the matrix for rubber ink utilizing the direct print process for the fabrication of 3D structures. In this article, which is a continuation of the work described in Kim and Choi (ref. 19), the goal is to print an ink with a high solid content. As synthetic latex has negligible amounts of solvent, the incorporation of this latex in the ink is expected to result in a high solid content in the printed structures. In addition, we aim to demonstrate that additive manufacturing techniques can be used for building tires (as comparable synthetic rubber combinations are used for manufacturing automobile passenger tires), which would aid in the development of a robust additive manufacturing process that can be used for tire manufacturing in the near future.

Material and methods

The rheological properties of rubber inks prepared from natural rubber and a synthetic rubber matrix were investigated previously in Kim and Choi (ref. 19). In that study, the properties of high solid content rubber inks used in the direct print process were evaluated in order to determine the ideal printing parameters, and the 3D printed specimens were subjected to vulcanization using heat treatment to create crosslinks in the specimens. In the present study, the focus is on the synthetic rubber latex ink formulations used to fabricate 3D printed structures by direct print, and then vulcanize the fabricated structures to facilitate heat induced crosslinking. The optimized test procedures from the study by Kim and Choi are adopted as a standard methodology for characterizing the rubber inks, determining the test setup and conducting the basic printing process for 3D printable rubber inks.

Materials

The liquid SBR (L-SBR) random copolymer rubber and liquid butadiene rubber (LBR) used in this study was obtained from Kuraray Company, Ltd. (Tokyo, Japan). Fumed silica (Cab-O-Sil M-5) to improve the rheological properties of the ink was purchased from Cabot Corporation (Boston, MA), and stearic acid activator was purchased from Sigma-Aldrich (St. Louis, MO). The vulcanizing agents and additives used in this study (sulfur, zinc oxide [ZnO], tetramethylthiuram disulfide [TMTD] and N-cyclohexyl-2-benzothioazole sulfenamide [CBTS]) were provided by Akrochem Corporation (Akron, OH).

Preparation of rubber inks

The rubber ink used in this study was prepared by adding L-SBR and LBR to a container in a 3:2 ratio, mixing the two rubbers at 2,500 rpm in a high speed mixer for 40 seconds with 10 phr of fumed silica. To enable vulcanization, a mixture containing 4 phr of ZnO, 1 phr of stearic acid, 4 phr of N cyclohexyl-2-benzothioazole sulfenamide (CBTS), 1 phr of tetramethylthiuram disulfide (TMTD) and 2.5 phr sulfur was mixed to homogeneity.

Setup and printing process for direct print system

The customized direct print setup used in this study, which was adopted from Kim et al. (ref. 20) is shown in figure 1. The setup

Figure 1 - direct print system: (a) close-up photo of dispensing syringe; (b) customized direct print setup

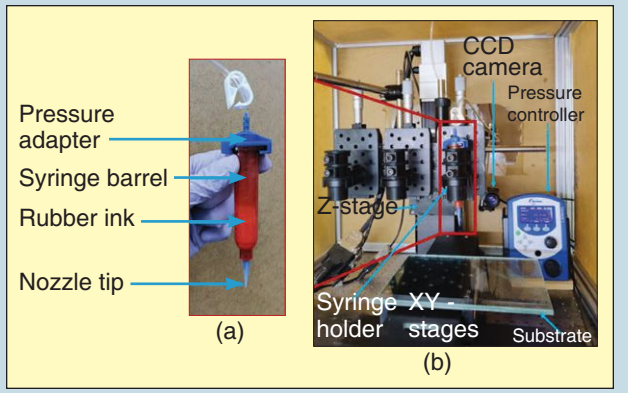

includes a pneumatic dispensing system (which consists of a pressure controller and dispensing syringes) and a motorized XYZ stage. Precision position control of the syringe tip was enabled by a PRO115 high resolution XYZ linear stage (Aerotech, Incorporated). ThorLabs model XR35C/M manual translation stages were installed on the Z stage for gap distance calibration between the substrate and the dispensing tips. Pneumatic dispensing was accomplished through the application of pressure by an Ultimus I pneumatic pump (Nordson EFD). To attain synchronized operation, the XYZ linear stages and pressure-controlled dispensing systems were controlled using G-code instructions sent through LabView systems engineering software (National Instruments).

A 3D model was designed using SolidWorks computer-aided design (CAD) software and exported in the stereolithography (.stl) file format. Open source slicing software (Repetier-Host from Hot-World GmbH) was used to generate the G-code instructions that contain the tool path and extrusion parameters needed for 3D printing. The layer thickness of 406 µm was adjusted based on the tip size. Infill density of 100% and a raster angle of 45°/45° were used for the print settings. The formulated ink was loaded into an Optimum syringe barrel (Nordson EFD) and remixed using a high speed mixer for 40 seconds at 2,500 rpm to remove any air bubbles in the material. Next, the syringe was placed on the XYZ stage and connected to the pneumatic pump for 3D printing. Various pressure and speed ranges were investigated to optimize the printing parameters for the ink.

Vulcanization process

A conventional rubber vulcanization technique that inserts sulfur crosslinks using heat treatment was adopted in this system by using the same additives as initiators, activators, crosslinking agents and accelerants. The high viscosity of the blended mixture enabled the additives (sulfur, stearic acid, zinc oxide, TMTD and CBTS) to diffuse homogenously. Vulcanization of the material was then achieved by thermal treatment of the sample at 140°C to 160°C for 20 minutes. After thermal treatment, the sample was left to cool to room temperature.

Figure 2 - rheology test plot for the ink conducted at 30°C

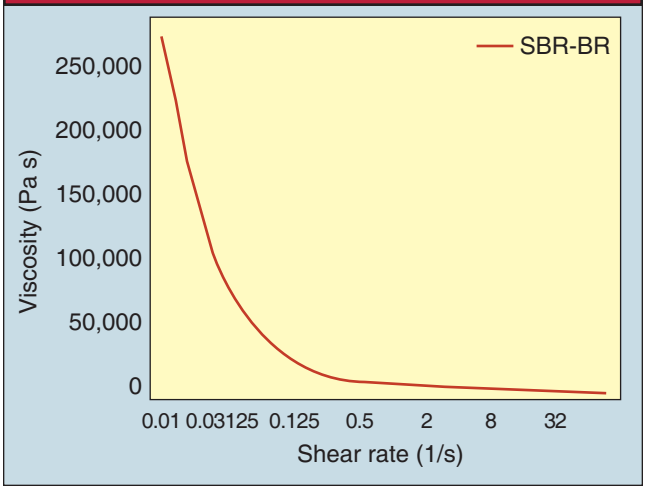

Figure 3 - printability test specimens: (a) microscope images of printed lines at 40x magnification; (b) serpentine shaped printability test samples

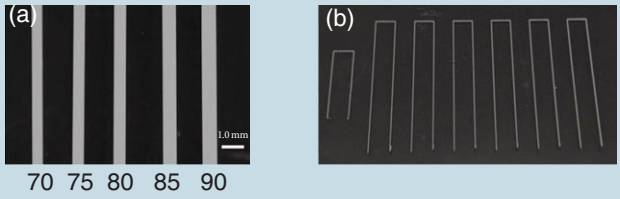

Results and discussion

Rheological properties

A TA Instruments ARES G2 rheometer was used for flow measurement under a strain rate from 0.01 to 100 s^{-1} at 30°C to measure the rheology of the rubber ink. The results shown in figure 2 indicate that the viscosity of the rubber ink depends on the shear rate, which is an important rheological property for improving the printing quality of the ink. The high viscosity of the 3D printable ink enabled the printed sample to hold its shape after extrusion from the nozzle tip, when the ink is no longer being subjected to any external stress. This reflects the shear thinning property of non-Newtonian fluids, in which the fluid viscosity decreases with the increase in shear stress (ref. 21).

Printability test of composite inks

A printability test was conducted to obtain the appropriate printing parameters for the rubber ink by operating the direct print system using various printing pressures and speeds to print basic lines. The inks were continuously printed for a length of 150 mm in the positive Y-direction and 150 mm in the negative Y-direction, with a distance of 10 mm between lines (along the X-direction). The widths of the printed lines were measured using a VHX-7000 digital microscope (Keyence Company, Osaka, Japan), and the results are shown in figure 3.

Next, lines of the rubber ink were printed at a constant speed while varying the pressure, and were printed at a constant pressure while varying the speed, where the gap height between the nozzle tip and substrate was set at 406 µm. The results for rubber ink printed at a constant speed of 1 mm/second at pressures ranging from 65 to 90 psi in increments of 5 psi are shown in figure 4a. The ink began to continuously dispense from the nozzle at 65 psi with an average line width of 500 µm (123% of the nozzle diameter). At 90 psi, the printed line width reached an average value of about 689 µm (169% of the nozzle diameter).

This finding indicates that a larger amount of material is dispensed as the pressure is increased. The results for rubber ink printed at a constant pressure of 85 psi at speeds ranging from 1 to 5 mm/second in 1 mm/second increments are shown in figure 4b. When using these print settings, the rubber ink had an average line width of 810 µm (close to 200% of the nozzle diameter) at a speed of 1 mm/second. At a speed of 5 mm/second, the average line width was reduced to 228 µm (56% of the nozzle diameter).

Tensile testing of printed specimens

For tensile testing of the rubber ink, ASTM D638 Type V dogbone specimens were 3D printed using direct print with 100% infill density, a nozzle tip with a diameter of 406 µm and a print speed of 5 mm/second. Figure 5 shows the 3D model for the tensile test specimen and a photograph of the printed specimens.

After the dogbone specimens were successfully printed, they were fully vulcanized by heating at 140°C to 160°C for 20 minutes prior to mechanical testing, which was conducted on an Instron 5582 universal testing machine. Tensile testing was accomplished for the specimens, and stress-strain curves were obtained (figure 6). The specimens had an average maximum tensile stress of 2.11 MPa and an elongation at break of ~400%.

Figure 4 - correlation plots between print parameters and width of the printed lines (a) at various pressures (b) at various speeds

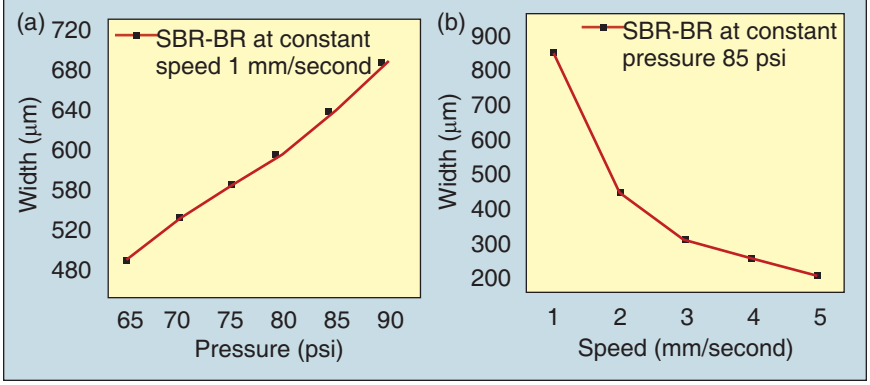

Figure 5 - ASTM D-638 Type V dogbone specimen: (a) 3D model (with dimensions in mm); and (b) photograph of vulcanized test specimens

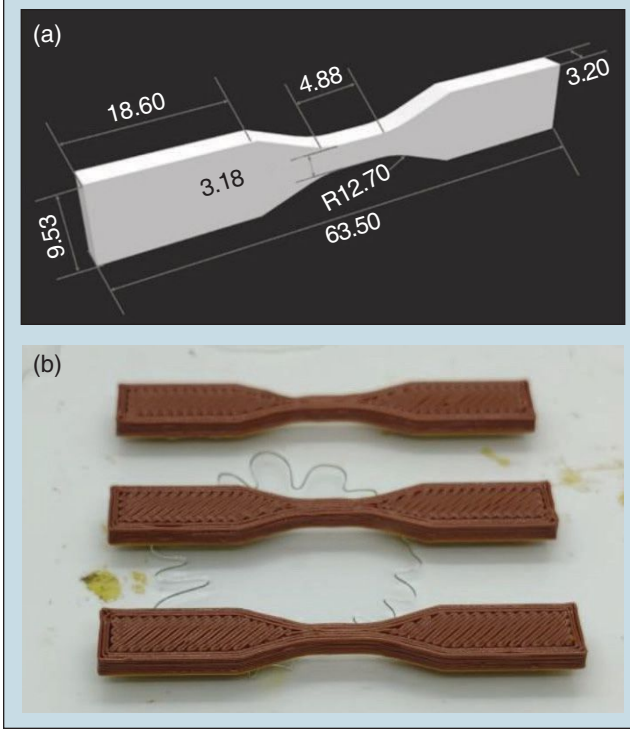

Figure 6 - stress-strain curves obtained in tensile tests conducted on dogbone specimens printed at 5 mm/second

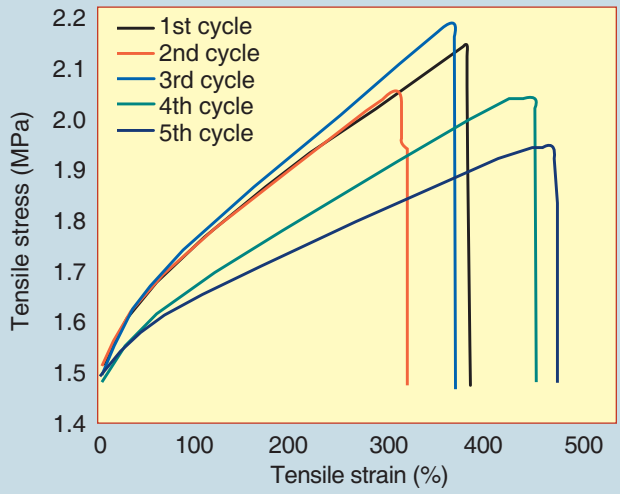

Dimensional accuracy analysis

The dimensional accuracy of a 3D structure is one of the most important factors that define the printability of a newly developed material. In this study, the accuracy assessment was accomplished by comparing the dimensions of each edge of the produced (green) part with those of the same part after it was vulcanized. First, a 3D model of a 1 cm^3 cubic structure was designed using SolidWorks (figure 7a). Next, five cube specimens for each ink were printed using a 406 µm nozzle tip and a 100% infill density. The printed green part is shown in figure 7b, and the inserted image demonstrates the XYZ direction of the cube. The dimensions of each green part were then measured using a VHX-7000 digital microscope (Keyence Company, Osaka, Japan). The cube specimens were fully vulcanized by heating at 140°C to 160°C for 20 minutes. After processing, the vulcanized specimen (also shown in figure 7c) was left to cool before measurements were obtained using the digital microscope. When the dimensions of the cube before and after vulcanization were compared (figure 8), it was found that the average change in volume was ~5.89%.

Demonstration of 3D structures printed using rubber ink

To demonstrate the freedom of fabrication, different 3D structures were designed and printed by the direct print process using the formulated rubber ink. The structures were built using the print parameters obtained from the printability test discussed in Section 3.2. CAD models of the 3D structures were first designed in SolidWorks (figure 9a). Next, G-code was generated using an open ource 3D slicing software in RepetierHost 3D printing software. After G-codes were obtained, the

Figure 7 - preparing cube specimens for dimensional accuracy analysis: (a) 3D model of the cube; (b) printed green specimen; (c) specimen after vulcanization

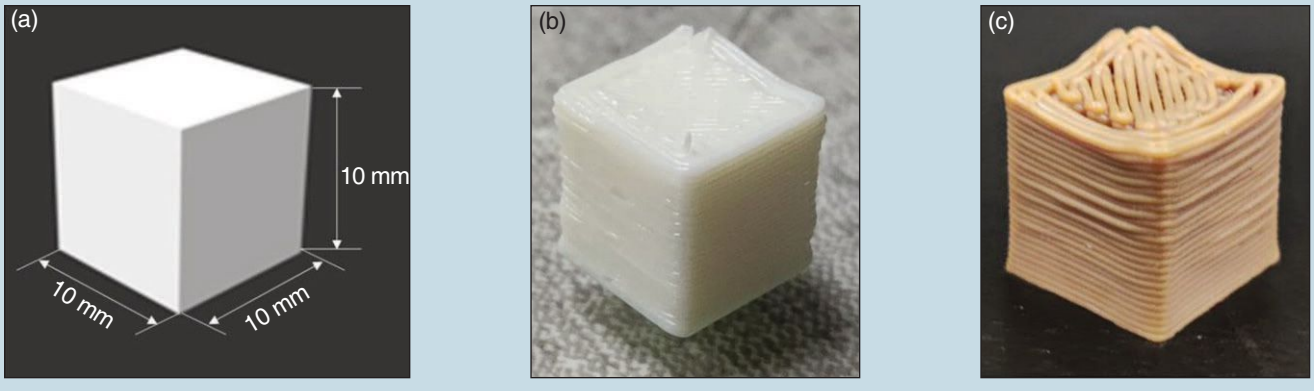

Figure 8 - dimensional accuracy test results for the printed cube

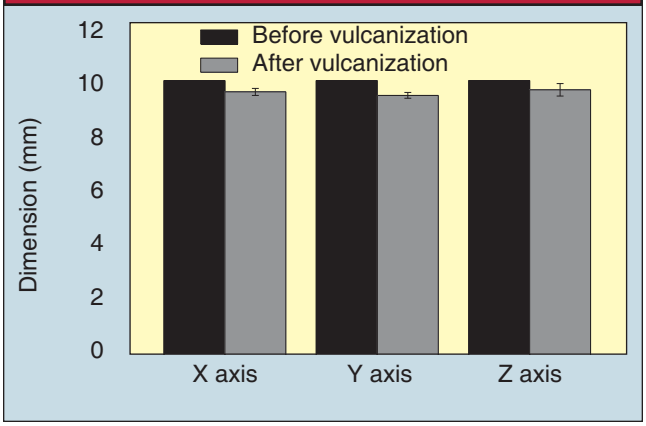

models were 3D printed using rubber ink (figure 9b). It was noted that due to the tackiness of the ink, the printed 3D structures had an uneven surface at some points on the top layer. The printed 3D structures were then vulcanized, and the resulting vulcanized parts are shown in figure 9c.

Discussion

Despite the fact that 100% infill density was used in the models, it is possible that air gaps (or pores) may be present in the printed parts. To confirm this, microscopy images of the cubic specimens were obtained using the digital microscope. It was found that the specimens had regularly distributed air gaps. These air gaps might have been generated after dispensing because of the circular shape of the filament, which may not allow the space between adjacent lines to be filled as the lines are printed.

Although the material dispensed from the nozzle may flow slightly, the spreading of the material would be limited due to the shear thinning property of the ink, and not all gaps between the lines would be filled. This issue could be partially solved by using a smaller syringe tip for dispensing and a smaller layer height in the design. Applications of this technology were examined that are closely related to tire tread manufacturing, where tread materials used for commercial tires have the tensile stress of ~16 to ~19 MPa and an elongation at break of ~280% to ~580% (ref. 22). The future direction of this work will include investigations of different materials, improving 3D printability and attaining mechanical properties close to commercially available products.

Conclusions

This study shows that synthetic rubber inks can be used for additive manufacturing and demonstrates the potential for rubber inks to be 3D printed using the direct printing technique. Conventional rubber manufacturing involves high pressure and high temperature processing, and cannot be used for fabricating customized parts unless the parts are made in very large batches due to the high cost of machinery dies and molds. Additive manufacturing helps overcome this circumstance by giving manufacturers the freedom to customize and produce parts on

Figure 9 - 3D structures fabricated by DP: (a) CAD models; (b) 3D printed green parts; and (c) final vulcanized parts

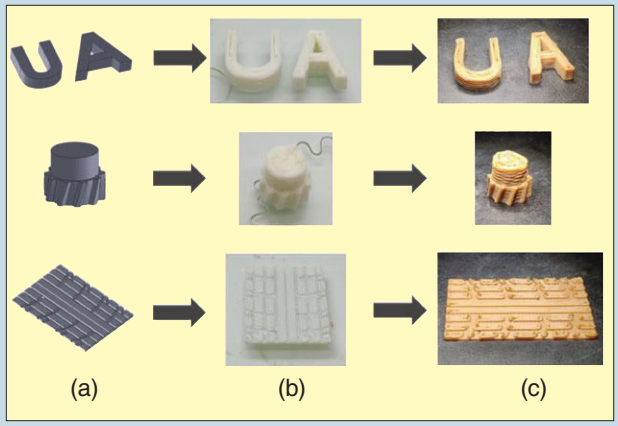

a small scale at a lower cost. The printability assessment of the ink shows that the pressure and print speed used in direct print can be adjusted to improve the print quality. In addition, an increase in the tensile strength and hardness of the printed part can be improved by varying the rubber blend to include additives (such as carbon black or ground tire rubber) to enable the printed parts to attain the properties of commercially available tire tread. The successful 3D printing and processing of the design models demonstrates that the rubber ink in this study can be printed, processed and used in future applications using the direct print process in the automotive and aerospace industries. The work conducted in this study was partially supported by research grants from the Center for Tire Research (CenTiRe) at The University of Akron. Future work will include further investigations to optimize the material properties of the rubber ink formulation, as well as to examine the effects of the material properties on the printability of the parts and the mechanical properties of the final processed parts.

References

1. D. Threadingham, W. Obrecht, W. Wieder, G. Wachholz and R. Engehausen, Rubber 3, Synthetic Rubbers, Introduction and Overview, Ullmann's Encycl. Ind. Chem., doi:10.1002/14356007.a23_239.pub5 (2011).

2. M. Michalovic, Destination Germany: A Poor Substitute, Polymer Science Learning Center, https://www.pslc.ws/macrog/exp/rubber/synth/methyl.htm (2000).

3. T.F. Marburg, "Review: [Untitled] buna rubber: The birth of an industry," Frank Atherton Howard, J. Econ. Hist., 8, pp. 228-228 (1948).

4. A.L. Gropman, "HA ~ U. S. Industry in World War II, McNair," Paper 50, Institute for National Strategic Studies, National Defense University, Washington, D.C. (1996).

5. L.H. Howland and R.W. Brown, "Recent developments in synthetic rubber latex," Rubber Chem. Technol., 34, pp. 1,501-1,520 (1961).

6. B. Berman, "3D printing: The new industrial revolution," Bus. Horiz., 55, pp. 155-162 (2012).

7. X. Wang, M. Jiang, Z. Zhou, J. Gou and D. Hui, "3D printing of polymer matrix composites: A review and perspective," Compos., Part B Eng., 110, pp. 442-458 (2017).
8. S.C. Joshi and A.A. Sheikh, "3D printing in aerospace and its long term sustainability," Virtual Phys. Prototyp., 10, pp. 175-185 (2015).
9. D. Böckin and A.M. Tillman, "Environmental assessment of additive manufacturing in the automotive industry," J. Clean. Prod., 226, pp. 977-987 (2019).
10. S.S.L. Chan, R.M. Pennings, L. Edwards and G.V. Franks, "3D printing of clay for decorative architectural applications: Effect of solids volume fraction on rheology and printability," Addit. Manuf., 35, 101335 (2020).
11. J.Y. Lee, J. An and C.K. Chua, "Fundamentals and applications of 3D printing for novel materials," Appl. Mater. Today, 7, pp. 120-133 (2017).
12. M. Lebedevaite, S. Ostrauskaite, E. Skliutas and M. Malinauskas, "Printing of thermosets," Polymers, 11, 116, doi:10.3390/polym11010116 (2019).
13. J.A. Lewis and G.M. Gratson, "Direct writing in three dimensions," Mater. Today, 7, pp. 32-39 (2004).
14. J.A. Lewis, "Direct ink writing of 3D functional materials," Adv. Funct. Mater., 16, pp. 2,193-2,204 (2006).
15. H. Yuk and X. Zhao, "A new 3D printing strategy by harnessing deformation, instability and fracture of viscoelastic inks," Adv. Mater., 30, pp. 1-8 (2018).
16. M. Lukić, J. Clarke, C. Tuck, W. Whittow and G. Wells, "Printability of elastomer latex for additive manufacturing or 3D printing," J. Appl. Polym. Sci., 133 (2016).
17. M.A. Quetzeri-Santiago, C.L. Hedegaard and J.R. Castrejón-Pita, "Additive manufacturing with liquid latex and recycled end-of-life rubber," 3D Print. Addit. Manuf., 6, pp. 149-157 (2019).
18. P.J. Scott, et al., "3D printing latex: A route to complex geometries of high molecular weight polymers," ACS Appl. Mater. Interfaces, 12, pp. 10,918-10,928 (2020).
19. M. Kim and J.W. Choi, "Rubber ink formulations with high solid content for direct ink write process," Addit. Manuf., 44, 102023 (2021).
20. M. Kim, D.G. Philip, M.O.F. Emon and J.-W. Choi, "Effects of hardness on the sensitivity and load capacity of 3D printed sensors," Int. J. Precis. Eng. Manuf., 223, 22, pp. 483-494 (2021).
21. B.A. Wolf, "Shear thinning: Determination of zero-shear viscosities from measurements in the non-Newtonian region," Macromol. Chem. Phys., 221, 2000130, doi:10.1002/macp.202000130 (2020).
22. M. Bijarimi, H. Zulkafli and M.D.H. Beg, "Mechanical properties of industrial tire rubber compounds," J. Appl. Sci., 10, pp. 1,345-1,348 (2010).